A location and movement dependent GNSS multipath error model for pedestrian applications

Andreas Lehner, Alexander Steingaß, Frank Schubert
Institute for Communications and Navigation, German Aerospace Center (DLR)

BIOGRAPHY

Andreas Lehner was born in Gmunden, Austria in 1973. He studied Mechatronics at the Johannes Kepler University in Linz. Since 2001 he is a research scientist at the Institute for Communications and Navigation at the German Aerospace Center DLR. In 2007 he received a PhD in Electrical Engineering from the University of Erlangen-Nuremberg. His research and project work focuses on analysis of multipath and interference effects in satellite navigation systems, and the design of inter-vehicle communication systems.

Alexander Steingaß was born in Mettmann, Germany in 1969. He received his Dipl. Ing. diploma in Electrical Engineering in 1997 (University of Ulm, Germany). Since then he has been a research scientist at the German Aerospace Center DLR - Institute of Communications and Navigation. He has been involved in several projects in the area of satellite navigation and location-dependent mobile services. In 2002, he was promoted to Dr. Ing. at the University of Essen.

ABSTRACT

In 2002 the German Aerospace Centre (DLR) performed a measurement campaign of the land mobile multipath channel in and around the city of Munich. From this data a channel model was derived that is synthesising the measured channel impulse response. It allows the realistic simulation of the multipath channel by approximating every single reflection. This model includes time variant reflectors approaching and receding in dependency of the azimuth and elevation of the satellite. All the signal processing had been realised independently of the transmitted signal. Therefore the usability for both, navigation systems (GPS as well as GALILEO) and wideband communication systems is given.

1. INTRODUCTION

The most significant problems to achieve an accurate navigation solution in urban and suburban environments with GPS or GALILEO are shadowing effects and multipath reception. Various channel models do exist for ground to ground communications (e.g. COST 207 for the GSM system). But there is still a lack of knowledge for broadband satellite to earth channels [1]. Therefore we performed a measurement campaign where we used a Zeppelin to simulate a satellite transmitting a 100 MHz broadband signal towards earth. To ensure a realistic scenario the signal was transmitted between 1460 and 1560 MHz just nearby the GPS L1 band. For the pedestrian channel measurements described in detail in [2], this signal was received via an antenna carried by a pedestrian on the side walk followed by a measurement van and was recorded using a regular time grid. The so gathered data was then passed through a super resolution algorithm to detect single reflections. In a further step we tracked the detected reflections in time and gained knowledge about the characteristics of any isolated reflection. This includes both Doppler shift and delay of the reflection. On top of this we gained knowledge about the direct path behaviour.

In this paper we will first describe the channel model itself to introduce the relevant parameters. In a separate section we will discuss the differences between the urban and the suburban environment for the pedestrian application case.

2. MEASUREMENT SCENARIO

During the measurements the whole range of elevations to the “satellite” from 5° to 90° was covered. For each elevation the receiver followed the same track, which covered typical pedestrian shopping streets and squares. To give an impression of the urban measurement area Figure 1 shows the Sendlinger Tor Straße in the city centre of Munich.

Figure 1: Snapshot of a shopping street scenario covered by the pedestrian measurements in the centre of Munich

3. DIRECT PATH

In an open environment the direct path is represented by the line of sight (LOS) transmission of the signal. In urban and suburban environments this LOS signal is often blocked so that the first received path is attenuated and possibly delayed with respect to the LOS. In urban and suburban environments we had been able to identify three major types of obstacles that influence the signal reception:

1. House fronts
2. Trees
3. Lamp posts

3.1 The influence of house fronts

When the LOS ray is going to be blocked by a house front the signal is obviously affected. Figure 2 shows the received direct path signal during the measurement when entering the shadow of a building. The x-axis indicates the distance from start. At about 3886 m the receiver antenna is entering the shadowed area. From this instance on the signal is strongly attenuated. This behaviour is well known from the so called "Knife Edge Model" [3]. In this model it is assumed that a planar wave is hitting a half-sided infinitively large plate. The calculated attenuation from this model is also displayed in Figure 2. From this comparison the similarity of measurement and model is obvious. Therefore the knife edge model is selected to model this effect. This process is motion dependent only.

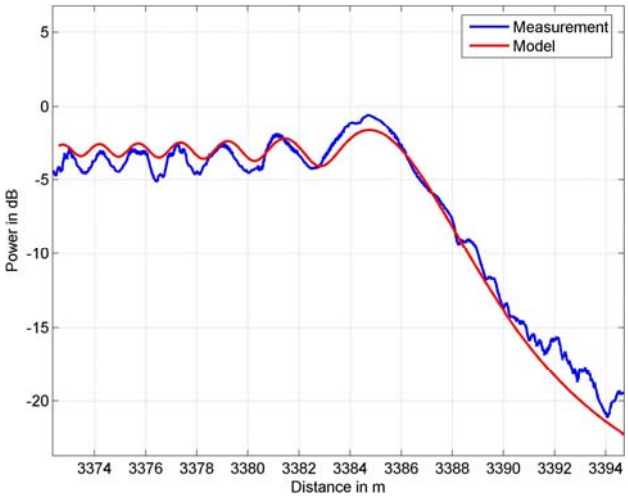

Figure 2: Diffraction by a house front – comparison of measurement and Knife Edge model.

3.2 The influence of trees

As it is shown in Figure 3 the LOS signal can be attenuated by trees. The measured process on the one hand side is dependent on the length of the LOS path being within the tree top, on the other hand side an additional process is visible caused by branches and leafs. In contrast to approaches where branches and leafs are modelled as very complex scatterers [4] we use a combination of an attenuating only cylinder modelling the transmission through the tree canopy and a statistical fading process modelling the branches and leafs. Both processes are motion dependent only.

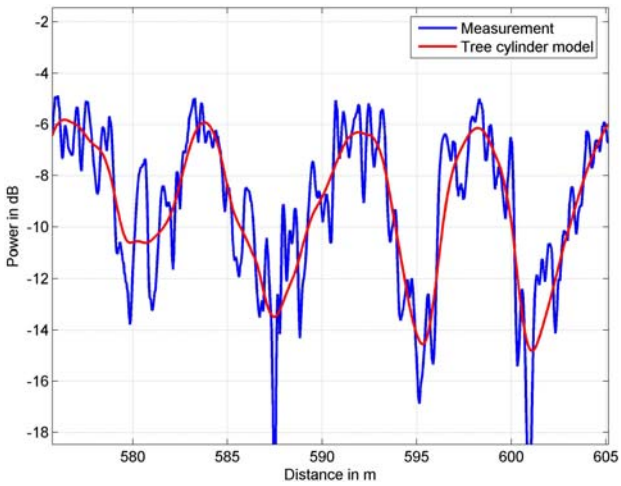

Figure 3: Signal attenuation by series of trees – comparison of measurement and cylinder model.

3.3 The influence of lamp posts

Surprisingly a lamp post has a strong effect on the direct signal. Figure 4 shows an example of a lamp post with a diameter D = 20 cm. When passing by such a post the strength of the signal begins to oscillate, goes down quickly in the direct shadow of the post and comes up again oscillating behind.

We model a lamp post with a "double knife edge model" where we assume two overlapping knife edge plates being present. One is reaching from $-D/2<x<\infty$ and the other is reaching from $-\infty<x<D/2$. Both edges are simulated separately and

then added coherently. Figure 4 shows the near perfect match of model and measurement. This process is also motion dependent only.

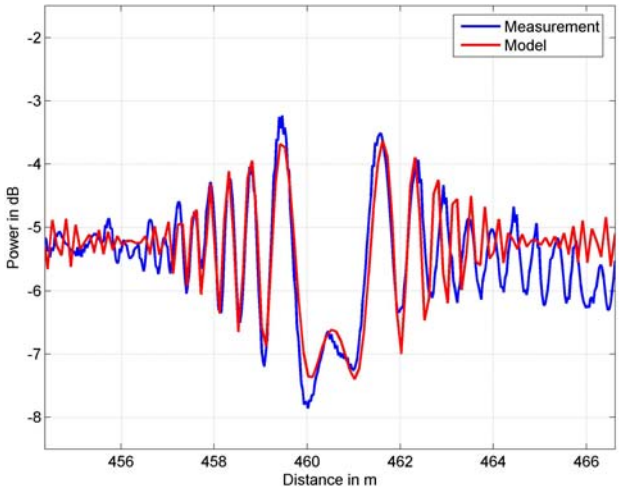

Figure 4: Direct path signal being affected by a lamp post – comparison of measurement and model

4. REFLECTED SIGNALS

In the measurement data many reflections appear in urban and suburban environment [5,6]. In contrast to ray tracing algorithms [7] we do not model a specific scenery. We assume reflections to be statistically distributed in the (x,y,z)-space and generate them statistically. In order to match the measured statistic we must take a closer look at the echo distribution.

4.1 Influence of the relative incidence angle

Let us assume a receiver to be at position RX, a satellite at position S and a reflector at position R. Then the relative azimuth receiving angle α is the angle at the receiver illustrated in Figure 5.

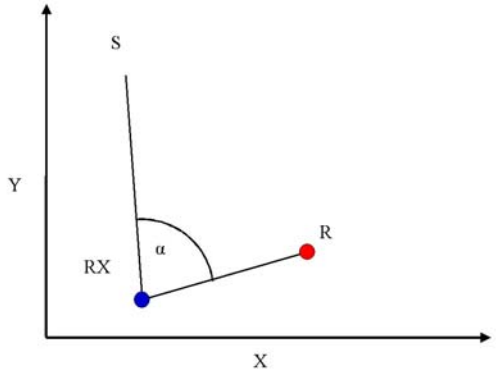

Figure 5: Definition of the angle α.

We can see a clear dependency on the relative azimuth angle in the urban measurement data (Figure 6) with a high likelihood for $60° < \alpha < 300°$.

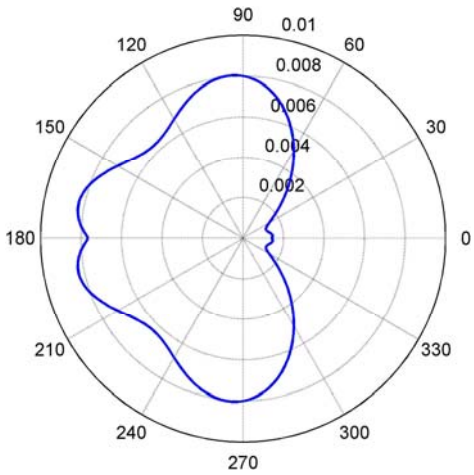

Figure 6: Likelihood distribution of the relative azimuth angle α in the urban pedestrian environment at 50° elevation.

For this figure we averaged over all occurring absolute azimuth angles θ by

$$\overline{p}(\alpha) = \frac{\sum_{\theta_i} \frac{p(\alpha|\theta_i)}{p(\theta_i)}}{\sum_{\alpha_i}\sum_{\theta_i} \frac{p(\alpha_i|\theta_i)}{p(\theta_i)}} \quad . \tag{1}$$

In contrast to the statistics for the urban car environment published in [8], where a clear maximum exists for $\alpha = 180°$, the incidence angle of reflected signals in the pedestrian case has another maximum around 90° and 270°, respectively. In urban car environments the rectangular structure of construction dominates. Due to this structure a corner reflector (see Figure 7) occurs very often. The main characteristic of this reflector is that a ray coming from a satellite is being reflected back into the satellite direction in the x-y plane. Its elevation is unchanged. Thus α is very likely around 180°. In a pedestrian zone environment on the other hand side many different kinds of reflecting objects exist. The fact that a pedestrian moves on the side walk rather than in the middle of the street, leads to a larger variation in back scatter angles of reflectors, because one moves closely between reflecting structures on the walls of houses and various objects separating the street from the side walk.

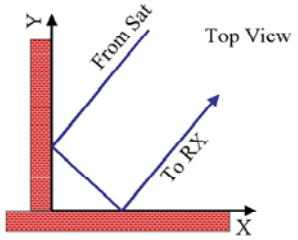

Figure 7: Corner reflector as it can be often found in urban environments.

4.2 Geometric occurrence of reflectors

Figure 8 shows the likelihood distribution of reflector positions in a top view. In this figure the receiver is moving in x-direction only. It can clearly be seen that the highest likelihood of receiving a reflector is when the reflector is on the right or on

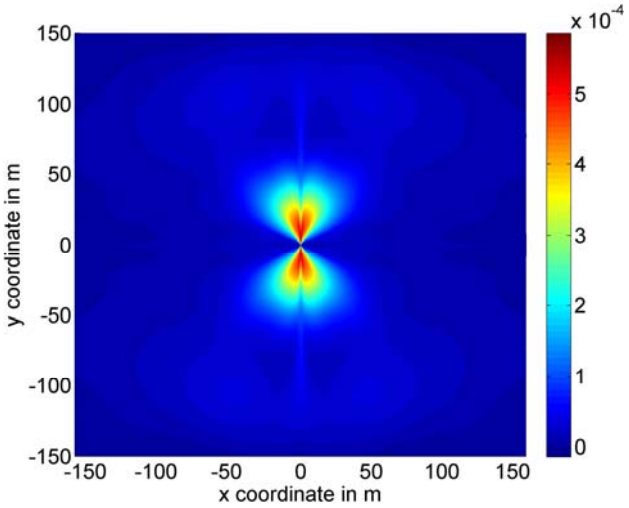

Figure 8: Likelihood of reflectors being at a certain 2-D position for 30° elevation in the urban pedestrian environment. Moving direction of the receiver is in x-direction only.

the left side. The likelihood of receiving a reflector from the front is close to zero. This as well on the first look astonishing result becomes more plausible when one has a side walk along a street in mind. It must be unlikely that a reflecting obstacle is in near front or back of the pedestrian; otherwise one would overrun it in the next moment. To calculate the common likelihood of a reflector being present at a certain position for a specific satellite azimuth and elevation we can multiply the statistically independent distributions shown in Figure 6 and

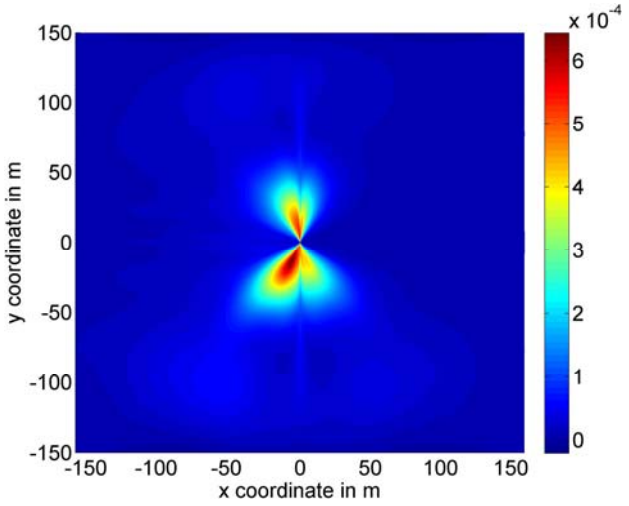

Figure 9: Common likelihood of reflectors being at a certain 2-D position for a satellite at 25° azimuth and 30° elevation.

Figure 8. The result of this operation is given in Figure 9, here the satellite position had been chosen at 25° azimuth. Comparing these results with the urban car case published in [8], the 2D position distribution in Figure 9 shows that the reflectors are much closer to the receiver, which affirms the statements in the previous section that many reflectors are very near on both sides of the side walk in the pedestrian case.

4.3 Life span of reflectors

In the measurement data the channel appears rapidly changing. Many echoes disappear and others appear at new positions. This process is highly correlated to the receiver speed. When the pedestrian with the receiver stops the reflections remain more or less static in the scenery. Therefore we defined a life distance of each reflector. This life distance is the distance the receiver is travelling until the echo disappears. Figure 10 shows a histogram of the echo life distances. It can be seen that the life distance of the reflectors is usually well below 1 m. This is clearly shorter than for the urban car environment in [8], where most reflectors exist along a motion path below 5 m. Therefore the channel is changing rapidly even though pedestrian movement is relatively slow.

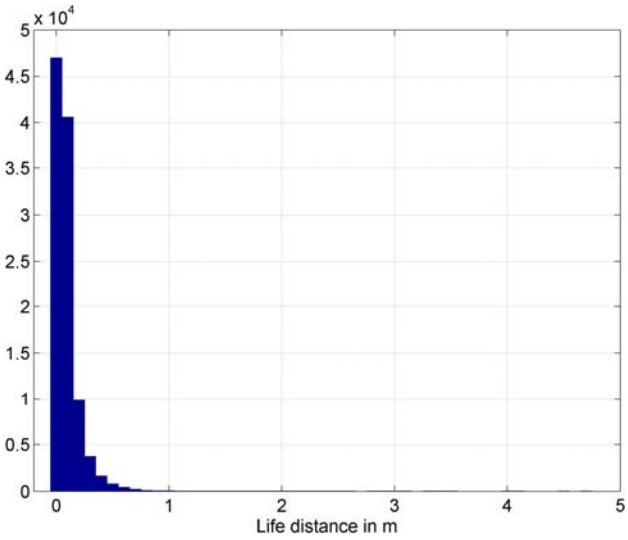

Figure 10: Histogram of the echo life distance in the urban pedestrian environment for 40° elevation

4.4 Mean power of reflectors

Figure 11 shows the power distribution in dependency of the relative reflector position. Since reflectors in the real world have a given geometrical size of course their distance plays a major role for the mean received echo power. In contrast to the urban car environment [8], where the most powerful reflections are coming only from the sides of the street, the distribution is less pronounced in the

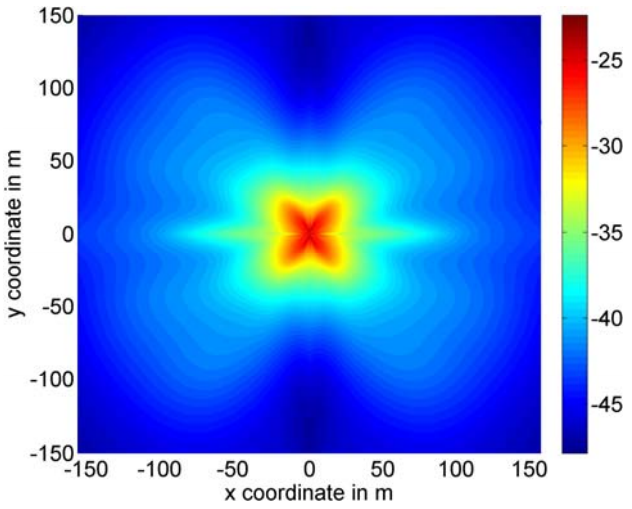

Figure 11: Mean echo power of the reflectors in dependency of their relative position for 50° elevation.

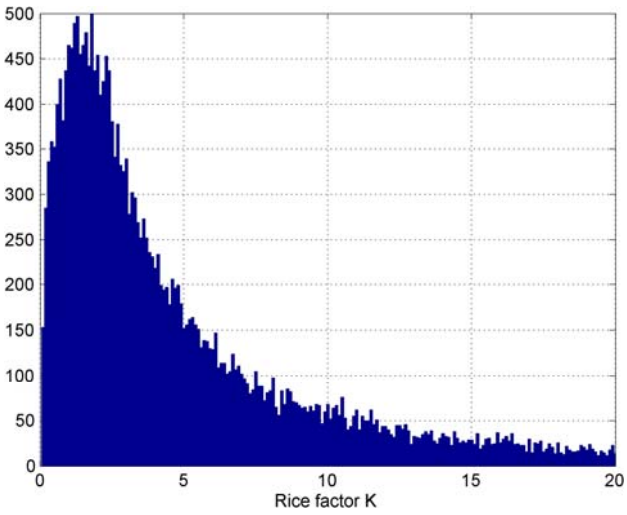

Figure 12: Rice factor histogram of the fading process of echoes in the urban pedestrian environment at 40° elevation.

pedestrian environment. With increasing distance the mean power of the reflections is decreasing. Beside the mean power map we have derived a power variance map (not shown) to allow a certain variation in this process, like we observed it in the measurements. For both, the urban car and pedestrian environment the average power level of echoes is approximately the same, where else it is about 3 – 5 dB higher in suburban environments as can be seen in [9].

4.5 Fading process of reflections

When a pedestrian walks through an urban or suburban environment the receiver moves through a quasi stationary field radiated by the reflectors. Therefore the receiver recognises a variation of the actual power of the reflector (see also Figure 13). Interesting enough this fading process does not even come to a stop when the pedestrian does not move. We assume that the channel is changing for example due to trees in the wind, other pedestrians and cars. Furthermore we found no correlation between this fading process and the receiver speed. Therefore we model this process time dependent only. The typical bandwidth of such a process is in the range of some Hertz. The deepness of the fades is expressed by the Rice factor K_{Rice}:

$$K_{Rice} = \frac{P_{const}}{P_{fad}}. \qquad (2)$$

It defines the ratio between the constant power P_{const} and the power of the fading process P_{fad}. Figure 12 shows the histogram of the Rice factor of the observed echoes in the urban pedestrian case for 40° elevation.

4.6 Time series characteristic of reflectors

Classical channel models like the GSM channel model [10] use time invariant path delays and model the change of the reflector over the time by the assumption that many echoes are received at almost the same path delay and their absolute azimuth is equally distributed. The resulting Doppler spectrum, the so called Jakes spectrum [11], is given by:

$$S(f_D) = \begin{cases} \dfrac{const}{\sqrt{1-\left(\dfrac{f_D}{f_{D\max}}\right)^2}} & \forall \ |f_D| < f_{D\max} \\ 0 & else \end{cases} \qquad (3)$$

This approach is feasible for narrow band systems like GSM but in a wide band system such as GPS/GALILEO we regard the modelling accuracy as insufficient. Figure 13 shows the sliding window Fourier transform of an isolated reflection. There it can be seen that the echo is best characterised by a trace in Doppler frequency. Within 1.6 s the Doppler frequency of the echo changes from +30 Hz to -5 Hz. In the same period the path delay of the echo changes. The variability of the echo signal is clearly dependent on the receiver speed. Therefore we implemented the channel model using a geometrical reflector representation. This means we initialise a reflector at a randomly chosen position (according to the measured statistics) and pass by with a receiver with the actual speed. Then both, path delay and phase of the echo can be calculated geometrically. This causes the main process to be motion dependent only. Figure 14 shows how a single reflector is modelled. In terms of the reflector the artificial scenery generates a continues series

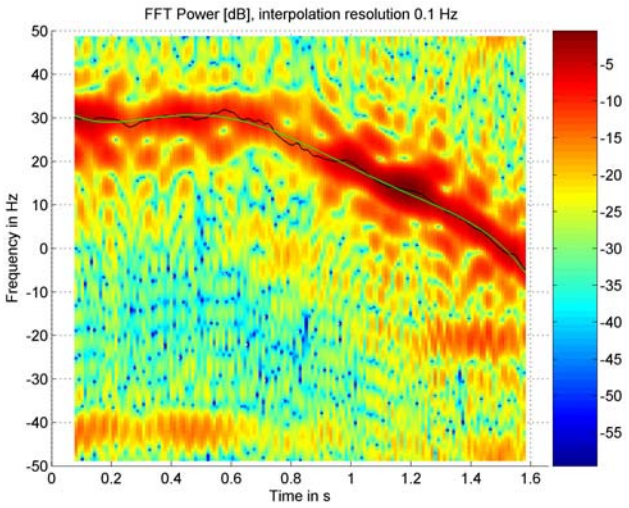

Figure 13: Sliding window Fourier transform of an isolated reflection.

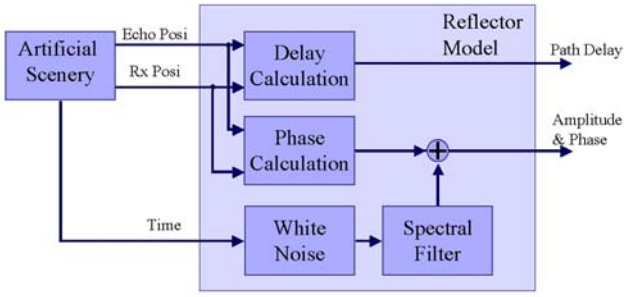

Figure 14: Model of an isolated reflector

of receiver positions according to the actual speed. The receiver is moving only in x-direction. To simulate turns the relative azimuth of the satellite is changed.

4.7 Number of echoes

During a walk through an urban pedestrian environment the number of echoes being received changes. For a navigation receiver that tries to estimate the channel impulse response (super resolution for multipath mitigation) a high number of reflections is a "high stress scenario". Other phases with a lower number of echoes are less critical. Besides the mean number of echoes it is therefore very important to exactly model this increasing and decreasing process. A sample of it is shown in Figure 15. Please note the relatively high number of echoes (sometimes more than 50) at the same time.

We had been able to detect two processes: An extremely narrow band process with high power and a lower powered wide band process. Their combination results in a very good approximation of the process. While the narrow band process models the changing character of the street, the wideband process resembles the changes on the level of house facades or trees.

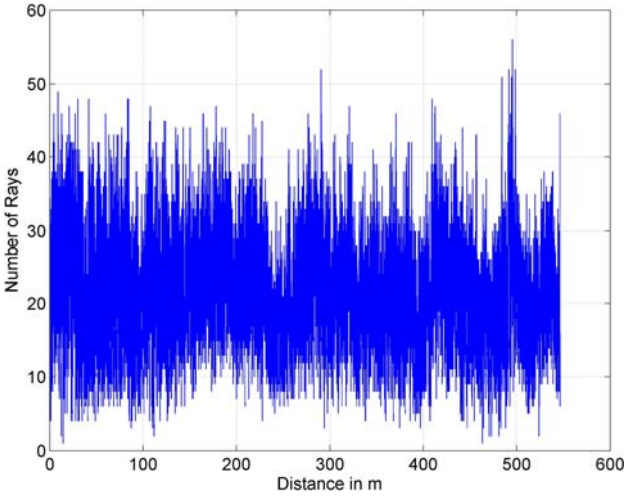

Figure 15: Number of coexisting echoes during a 10 minute walk trough an urban pedestrian environment at 40° elevation.

5. SATELLITE CHANNEL MODEL

The block diagram in Figure 16 gives an overview of the implemented satellite-to-earth multipath channel model. The x-coordinate and the relative satellite azimuth are derived from the user speed, user heading and satellite azimuth as explained in section 4.6. This drives the artificial scenery

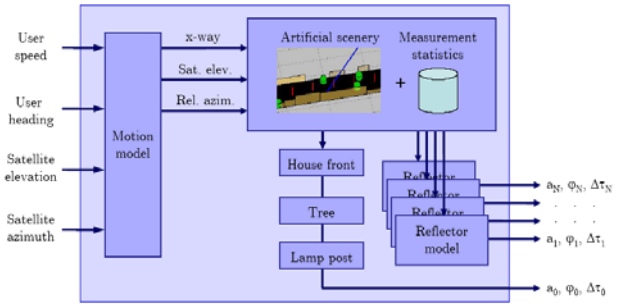

Figure 16: Block diagram of the channel model.

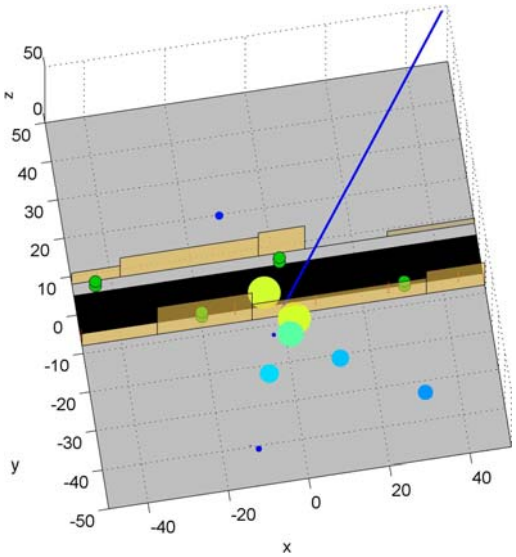

Figure 17: A picture of the artificial scenery with house fronts in brown, green cylindrical trees and red poles.

depicted in Figure 17, where house fronts, trees and lamp posts affect the direct path. Controlled by a number of echo generator the actual amount of reflections is created in the scenery at positions according to the likelihood distribution. These reflector positions are represented by the bubbles in Figure 17, where the echoes power is coded by size and colour. The reflectors power, bandwidth, rice factor and lifespan are taken from the statistics. Their delay and phase is therefore changing according to this statistical parameters and according to the receiver movement relative to the reflector position. In Figure 18 - Figure 21 an example output of the channel model is given. In this scenario the pedestrian moves with a variable speed (using a sin(t) like stop and go function) through an urban environment. At 4.7 s the speed is nearly 0 km/h. In Figure 19 the Doppler shift of each echo is shown. The red dotted line is the theoretical limit for the Doppler shift given by

$$f_{Doppler} = \frac{\vec{v} \cdot \left(\overrightarrow{RX} - \vec{S}\right)}{c_0} f_C \qquad (4)$$

where $\vec{v}$ is the speed vector of the user, RX is the receiver position, f_C is the carrier frequency, S is the satellite position and c_0 is the speed of light. In this figure and in the detail in Figure 21 one can determine isolated echoes changing their Doppler during their life distance, for example the dark green coloured echo lasting from 0.2 – 1.7 s changing the Doppler from about -4 to -8 Hz as the receiver moves ahead. The changing width of the lines in Figure 21 represents the changes in the power of the echoes. The fast Doppler variation is a result of the modelled time dependent process in the order of a few Hertz, whereas the Doppler trend (Doppler shift) is the deterministic process according to the geometrical change when the receiver moves through the scenery.

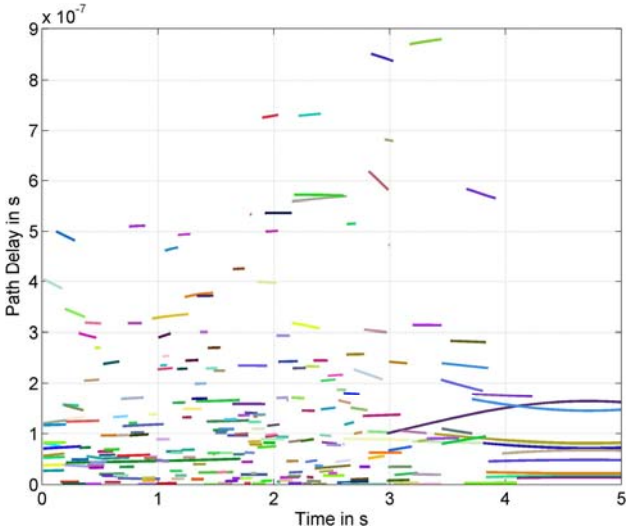

Figure 18: Example of generated echoes. Plotted is the path delay of the reflections over time.

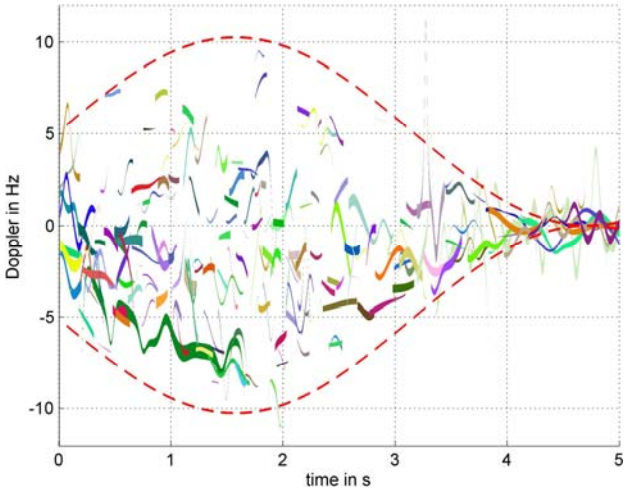

Figure 19: Example of generated echoes. Plotted is the Doppler of the reflections over time.

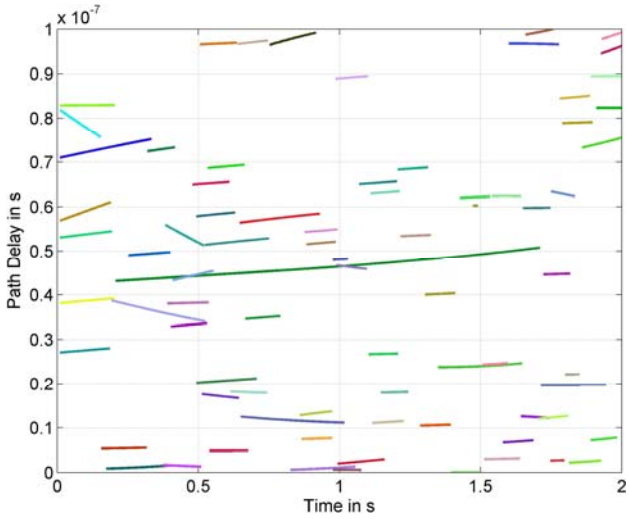

Figure 20: Detail of **Figure 18**.

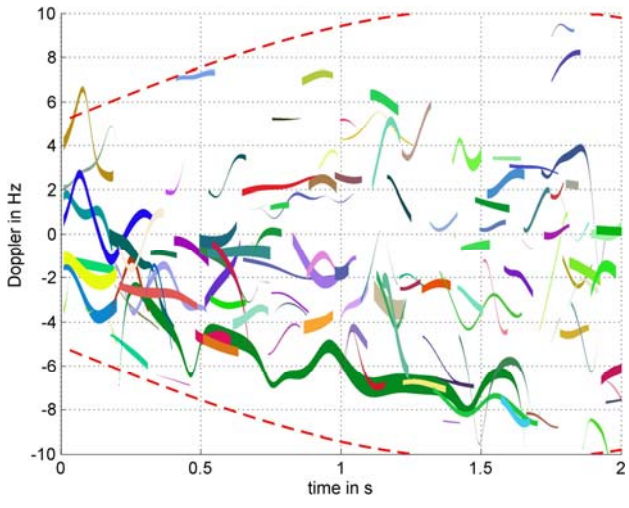

Figure 21: Detail of **Figure 19**.

The rapid changes in the channel are visible within the displayed period of around two seconds, where many echoes die and others are generated. Around the standstill the channel does not change much - clearly visible by the low Doppler bandwidth and the long lasting echoes (long lines) in Figure 18. In this situation only the time driven fading process is changing the channel. Neither an echo is terminated nor a new one generated in this situation. Furthermore one can see regions where more echoes are present than in others.

Due to this precise modelling of reflections new receiver algorithms for e.g. multipath mitigation can be tested in very realistic simulations now. An important improvement compared to regular statistical models is the geometrical reflector representation which guarantees the realistic delay and phase correlation among the occurring echoes.

6. COMPARISON BETWEEN URBAN AND SUBURBAN PROPAGATION

The direct comparison between the urban and suburban propagation case for pedestrian applications is done for the most relevant parameters:

- Mean power of the reflections,
- geometrical distribution,
- relative angle distribution,
- and number of coexisting echoes.

Figure 22 shows the mean power of reflections in dependency of their position. It can be seen that in the suburban case the echoes are stronger than in the urban case (note the colour bar in dB). Comparing Figure 26 and Figure 29 this seems to be true for all elevations above 10°.

Figure 23 shows the likelihood distribution of the echoes in the x-y plane. It can clearly be seen that for an elevation of 50° the echoes are wider distributed in the urban case. The comparison of Figure 27 and Figure 30 is supporting this finding especially for high elevations. For elevations below 50° the distributions are very similar. We believe that this is a result of the more random and more open structure in suburban pedestrian areas, in contrast to the very regular and rectangular structures (e.g. roofs) in the urban area.

Figure 24 shows the distribution of the relative angle of arrival for the two environments at 50° elevation. Again we see clear differences. In the urban case the distribution is much wider and we see the characteristic side maxima around 90° and 270°, which are not present in the suburban environment. As well the comparison for different elevations in Figure 28 and Figure 31 shows this feature of the urban pedestrian environment, especially for elevations above 30°.

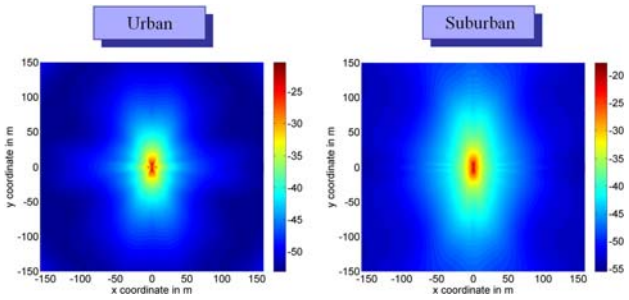

Figure 22: Mean power of echoes in dependency of the reflector position at 70° elevation – comparison urban and suburban pedestrian environment.

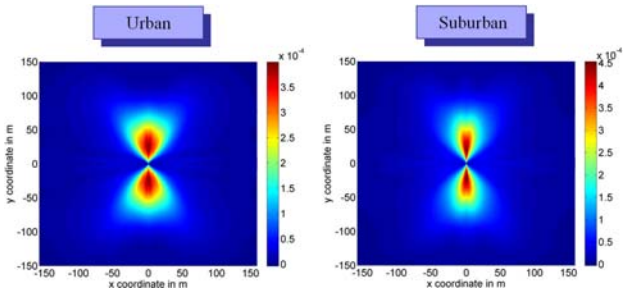

Figure 23: Likelihood of reflector occurrence in dependency of their position at 50° elevation – comparison urban and suburban pedestrian environment.

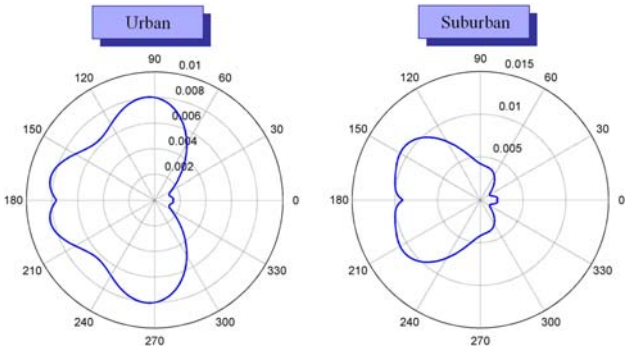

Figure 24: Distribution of the relative incidence angle at 50° elevation (see Figure 6) – comparison urban and suburban pedestrian environment.

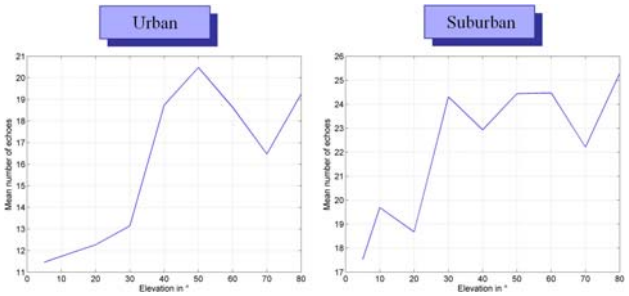

Figure 25: Number of coexisting echoes – comparison of urban and suburban pedestrian environment.

ELEVATION DEPENDENT ANALYSIS – URBAN PEDESTRIAN

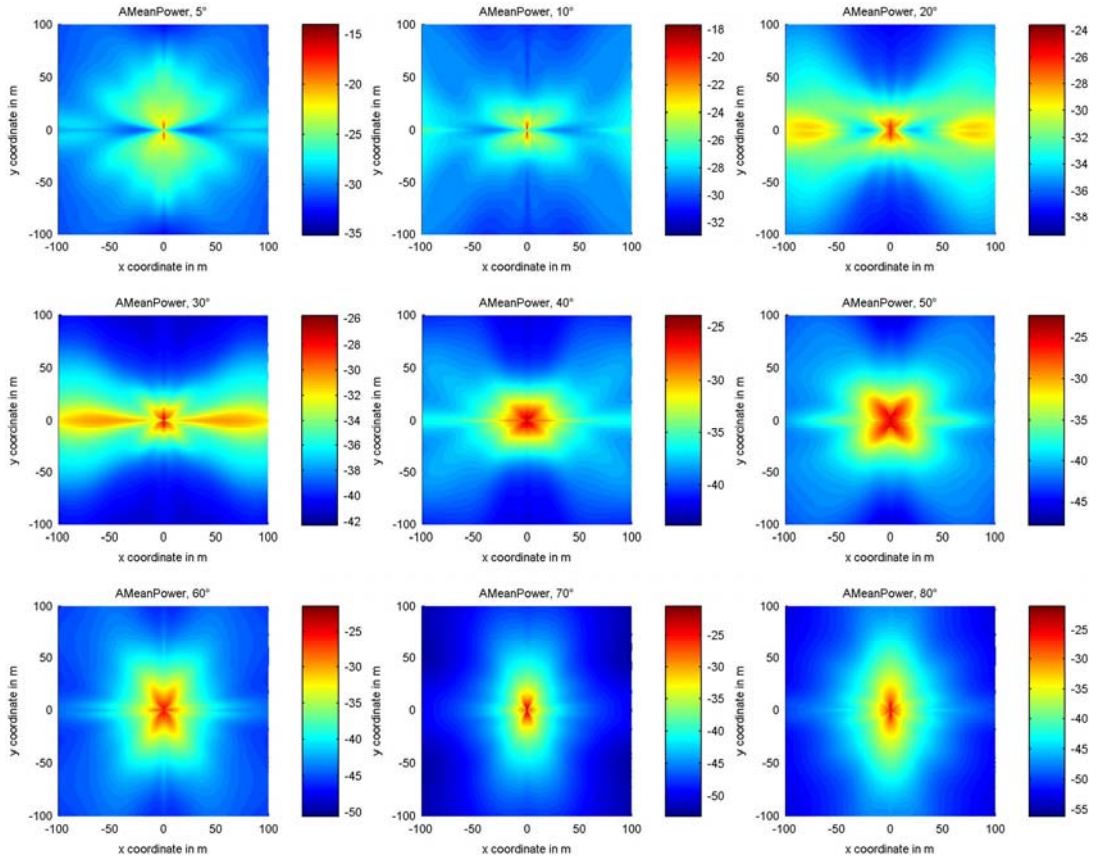

Figure 26: Mean power of reflections in dependency of their 2-D position and the satellite elevation – urban pedestrian

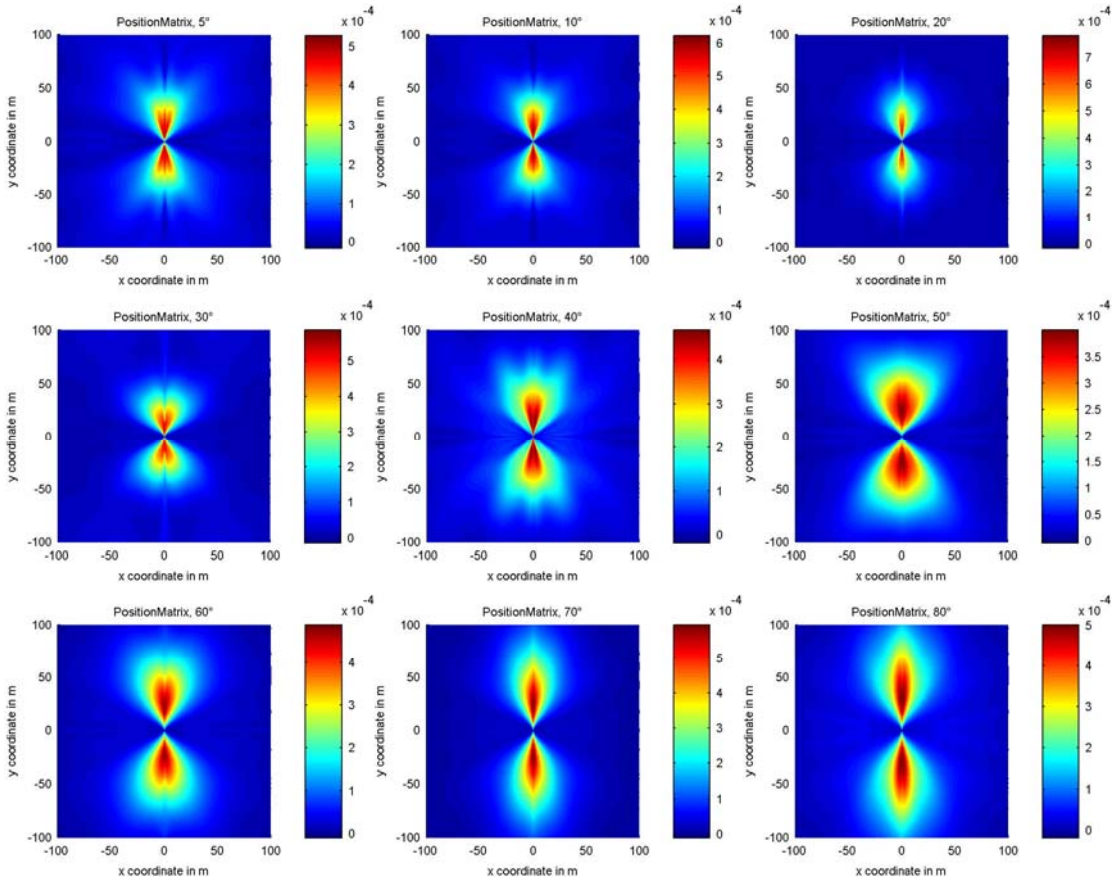

Figure 27: Likelihood of reflector 2-D position in dependency of the satellite elevation – urban pedestrian

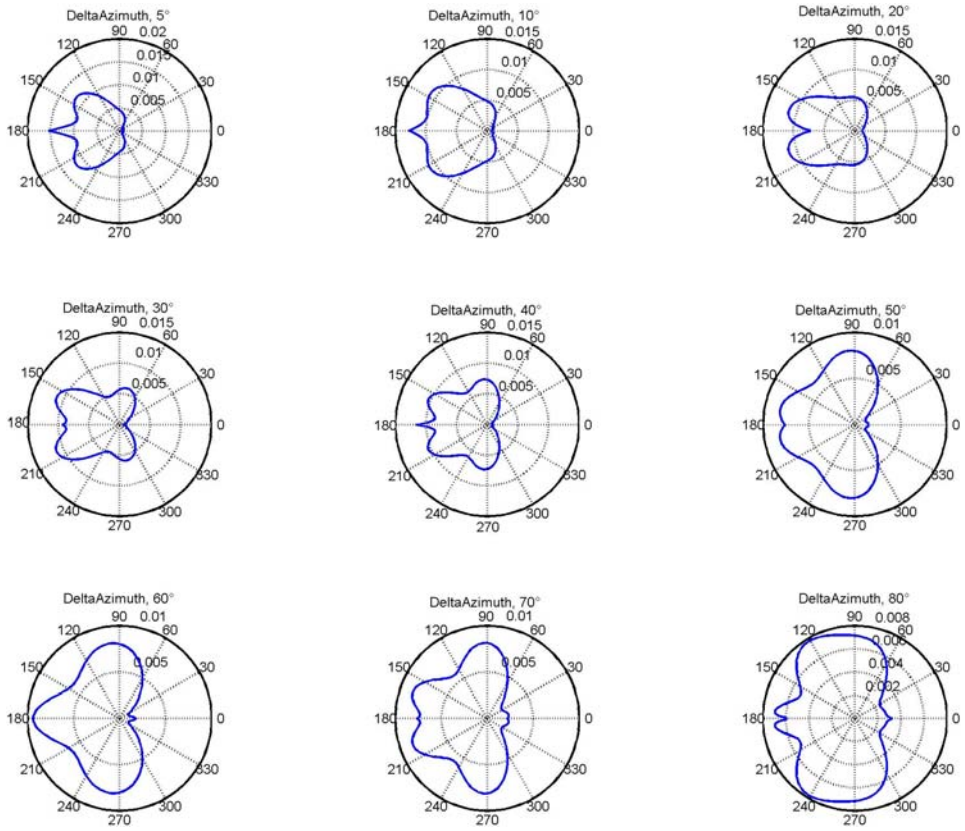

Figure 28: Distribution of the relative incidence angle in dependency of the satellite elevation – urban pedestrian

ELEVATION DEPENDENT ANALYSIS – SUBURBAN PEDESTRIAN

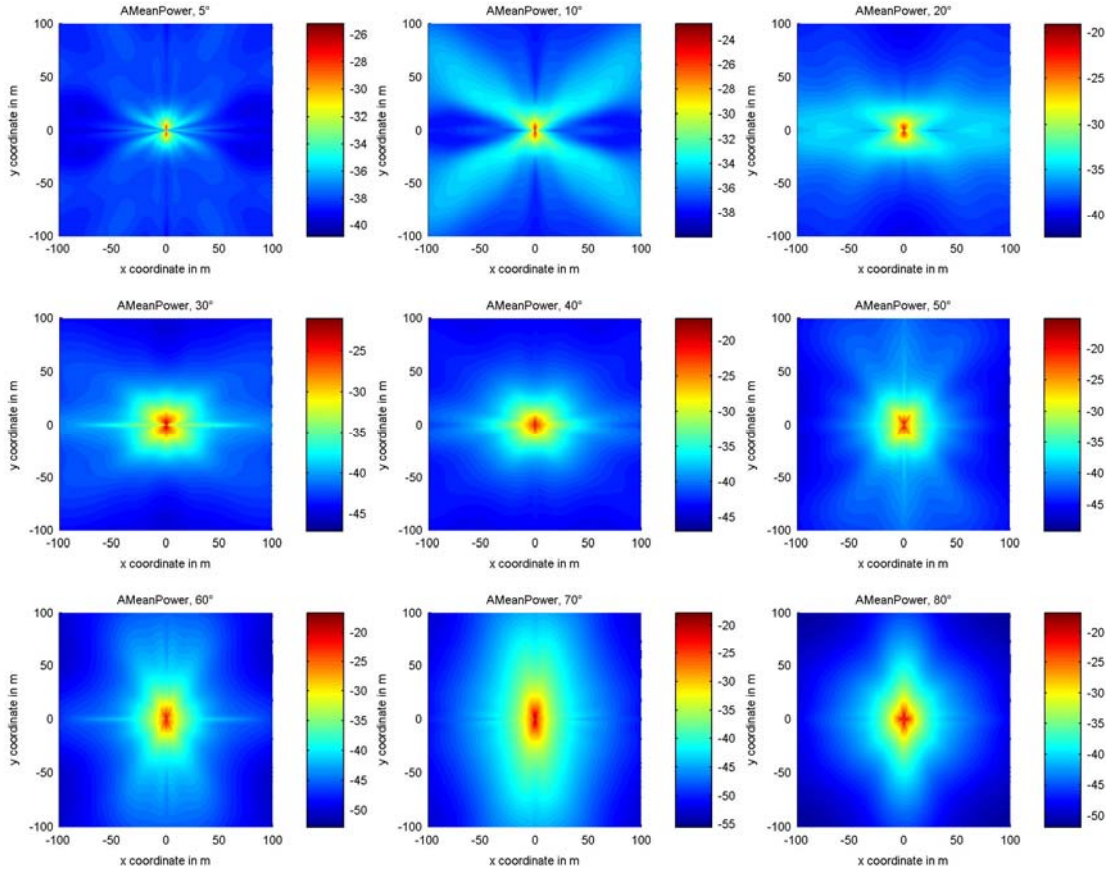

Figure 29: Mean power of reflections in dependency of the 2-D position and the satellite elevation – suburban pedestrian

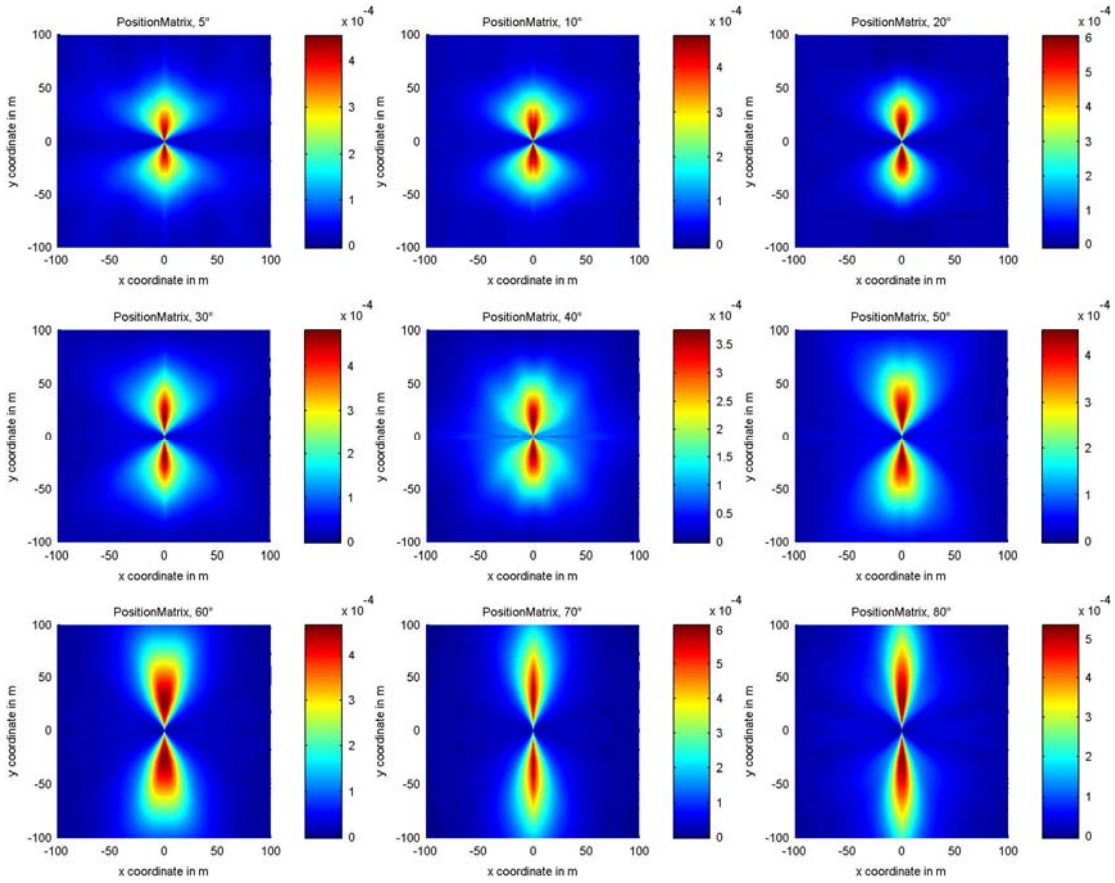

Figure 30: Likelihood of reflector 2-D position in dependency of the satellite elevation – suburban pedestrian

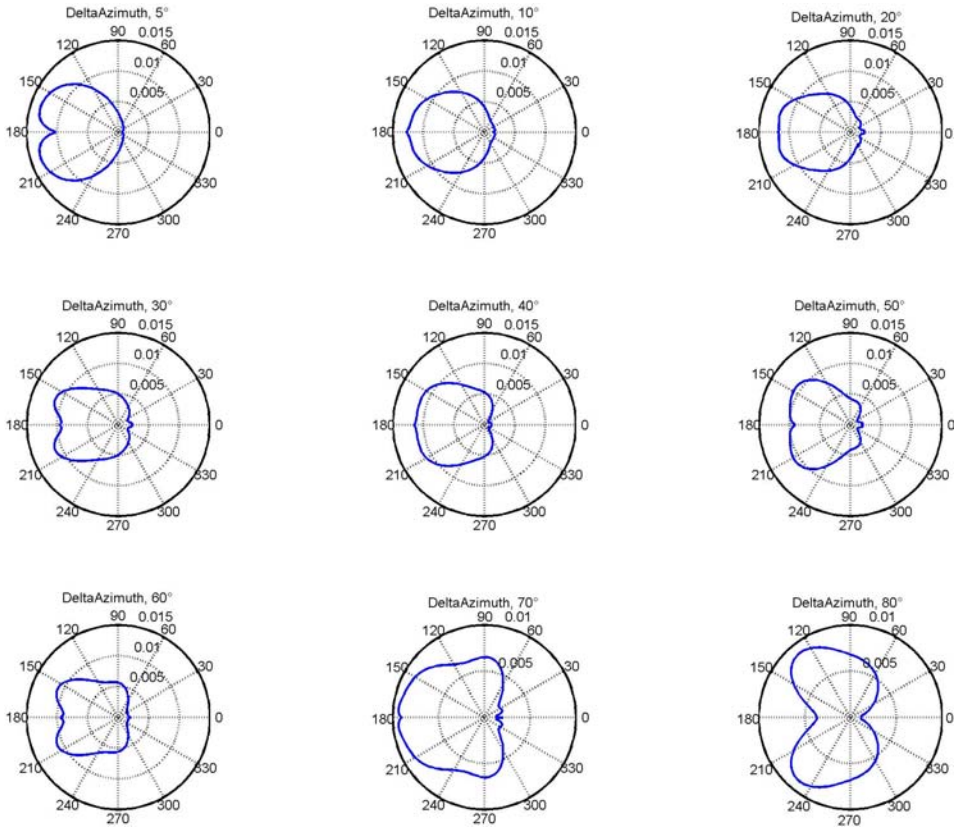

Figure 31: Distribution of the relative incidence angle in dependency of the satellite elevation – suburban pedestrian

In Figure 25 the mean number of coexisting echoes is plotted for both cases in dependency of the elevation. This comparison shows that in the suburban case there are more reflections at the same time. Note that the number significantly increases at 30° (suburban) and 40° (urban), respectively. The reason for this effect is the lower height of houses in the suburban environment. In fact the geometric relation between street width and house height in combination with the user position on the road plays a major role. The number of coexisting echoes starts to increase when the elevation is high enough to allow for a LOS. We believe that in this case more echoes from the surrounding are received, which would be blocked at low elevations. As a matter of fact we can see this change also in other channel parameters. In Figure 26 to Figure 31 we can observe that the character of the distributions also changes as the elevation becomes larger than 30° to 40°.

7. SUMMARY

In this paper we have presented our channel model for satellite-to-earth propagation and we have shown and compared the statistically relevant parameters for pedestrian applications in urban and suburban environments. This novel land mobile multipath channel model is based on a new approach: The combination of statistical data from measurements with a deterministic scenario. The deterministic scenario is used for the direct path modelling. This includes effects such as shadowing by house fronts, tree attenuation and diffracting lamp posts. The reflections of this channel model are generated statistically in the geometric scenario. Their generation is driven by data obtained from the measurement only. The model includes:

- Elevation changes,
- azimuth changes,
- speed changes,
- and a variable number of reflectors.

The model is available for download:
http://www.kn-s.dlr.de/satnav/

REFERENCES

[1] Schweikert R., Wörz T.: "Signal design and transmission performance study for GNSS-2", Tech. note on digital channel model for data transmission, ESA, 1998.

[2] Lehner A., Steingaß A.: "Measuring GALILEO's Channel - The Pedestrian Satellite Channel". Satellite Navigation Systems: Policy, Commercial and Technical Interaction, Proceedings of an International Symposium ISU 2003, Kluwer Academic Publishers, The Netherlands, May 26-28, 2003, pp. 159-166, ISBN: 1-4020-1678-6

[3] Orfanidis J. S.: "Electromagnetic Waves and Antennas", Internet www.ece.rutgers.edu/ orfanidi/ewa, Rutgers University, June 2004.

[4] Yvo L. C. de Jong and Matti H. A. J. Herben: "A tree-scattering model for improved propagation prediction in urban microcells", IEEE Transactions on Vehicular Technology, pages 503–513, March 2004.

[5] Steingass A., Lehner A.: "Measuring the navigation multipath channel a statistical analysis", ION GPS 2004 Conference Long Beach, California USA, September 2004.

[6] Steingass A., Lehner A.: "Measuring Galileo's multipath channel", Global Navigation Satellite Systems Conference (GNSS2003), Graz, Austria, 2003.

[7] Esbri-Rodriguez O., Konovaltsev A. and Hornbostel A.: "Modeling of the GNSS directional radio channel in urban areas based on synthetic environments", Proceedings of ION NTM, Jan. 2004.

[8] Lehner A., Steingaß A.: "A novel channel model for land mobile satellite navigation". Institute of Navigation Conference ION GNSS 2005, Long Beach, USA, September 13-16, 2005.

[9] Lehner A., Steingaß A.: "Time series multipath modelling of suburban environments in landmobile satellite navigation". 2nd European Conference on Antennas and Propagation EuCAP 2007, Edinburgh, Scotland, November 12-16, 2007.

[10] COST 207 WG1: "Proposal on channel transfer functions to be used in GSM tests 1986", Technical report, CEPT Paris, 1986.

[11] Jakes W. C.: "Microwave Mobile Communications", John Wiley & Sons, Inc., New York, 1974.